Article

Identification of Wind Power Potential for Phases I and II Wind Farms in Brazil Using Various Statistical Estimation Models and WAsP

Gerardo L. Augusto [1,2,*], Laurence A. Gan Lim [1,2], and Keith Lam [3]

[1] Department of Mechanical Engineering, De La Salle University, Manila 1004, Philippines
[2] Wind Tunnel Laboratory, De La Salle University—Laguna Campus, Binan 4024, Philippines
[3] Avantis Energy Limited, Hong Kong SAR, China
* Correspondence: gerardo.augusto@dlsu.edu.ph
Received: 19 May 2025; Revised: 18 August 2025; Accepted: 15 September 2025; Published: 19 September 2025

Abstract: The less promising but still feasible sites for wind farm development are the areas between the State of Santa Catarina and the State of Rio Grande do Sul, Brazil. To better understand the available wind energy potential in the region, a wind resource assessment was carried out for Phases I and II wind farms in Santa Vitoria do Palmar, Brazil. The data used for wind analysis were collected from April 2007 to March 2008 at a meteorological mast height of 101 m. Ten-minute data on wind speed, standard deviation, wind direction, relative humidity, environmental temperature, and pressure were recorded. Analytical estimation models were employed to determine the Weibull parameters necessary for calculating the annual average wind speed, mean power density, cumulative distribution, and probability density functions of the wind regime. The probability density function statistical results were analyzed at two different heights—the reference height of 101 m and the hub height of 80 m. The outcomes were then compared with the WAsP numerical output. The analysis showed that the energy pattern factor method has a confidence level above 97.5% with a correlation coefficient of 100%. The calculation results indicated that the annual mean wind speed at 80 m hub height was 8.10 m/s. This suggests that the site is suitable for IEC 61400-1 Ed.3 Class II wind turbine generators. The characteristic wind turbulence at a reference height of 101 m was classified as IEC Subclass C. Among the selected wind turbine generators, the 2.5 MW AV928 has the highest capacity factor at 41.22% and the lowest levelized energy cost of US$44.36 per MWh. Additionally, WAsP was utilized to numerically estimate the net annual energy production for the locality. Based on the proposed arrangement of wind turbines, the predicted net annual energy production, considering the wake loss effects, is expected to be 104.92 GWh/year for Phase I and 456.89 GWh/year for Phase II of the wind farms.

Keywords: wind resource assessment; statistical estimation models; annual energy production; cost analysis; WAsP analysis

1. Introduction

Carbon dioxide (CO_2) emissions have been increasing worldwide, mainly due to human activities such as burning fossil fuels, deforestation, and land use changes, as well as industrial processes. The primary source of carbon dioxide emissions is the burning of fossil fuels for transportation, electricity, and manufacturing [1]. As global energy demands keep rising, reliance on these carbon-rich fuels also grows. To effectively reduce worldwide carbon dioxide emissions, a comprehensive and multi-faceted approach involving various sectors and stakeholders is essential.

Transitioning to renewable energy sources is widely seen as the main solution for lowering global CO_2 emissions. Renewable energy creates electricity without releasing harmful CO_2 or other greenhouse gases into the atmosphere. Recent advances in renewable energy technology have made it more efficient and affordable, leading to broader deployment and adoption worldwide. Wind energy is one of the most actively developed and explored sources among these technologies. According to the International Renewable Energy Agency (IRENA), the average annual installation of offshore wind power plants since 2015 has increased by 24.34%, while onshore wind power plants experienced an 11.24% rise, reaching a total installed capacity of 1132.84 GW globally by 2024, as shown in Figure 1. The top five countries contributing to wind energy technology growth are China at

46.06%, the United States at 13.52%, Germany at 6.43%, India at 4.25%, and Brazil at 2.91%. Among these, Brazil has the highest annual wind energy installation increase rate at 17.80%, followed by China at 16.79% and France at 10.20%, beginning in 2015, as shown in Figure 2 [2].

The growth of Brazil's wind energy production is driven by the government program called the Program for Incentive of Alternative Electric Energy Sources, introduced in 2009 to promote wind, biomass, and hydroelectric power. As a result, 71 projects were approved for bidding for energy supply in Brazil in December 2009. The contracts, totaling 1800 MW, began in July 2012 with a 20-year supply period. Brazil's wind power potential could exceed 145,000 MW [3]. Currently, Brazil's total installed wind energy capacity is 32,959 MW, which accounts for just 22.73%. However, utilizing wind turbine technology still requires a thorough wind resource assessment to accurately predict the flow regime type and the potential energy available at a specific site.

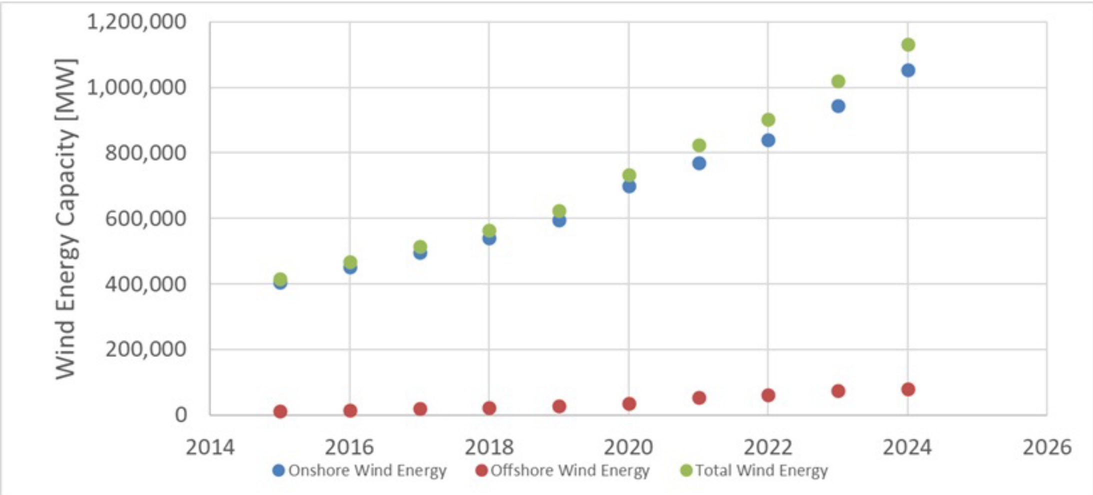

Figure 1. Wind energy capacity generation for onshore and offshore wind turbine generators globally.

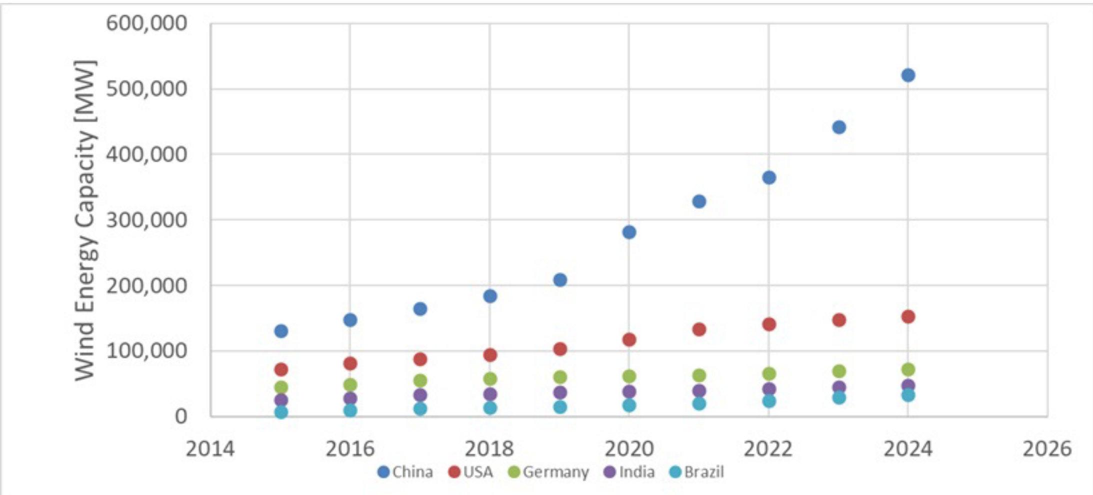

Figure 2. The top five nations contributed to wind energy generation.

Wind resource assessment is crucial for evaluating the viability of a potential wind energy project at a particular location. This data is vital for developers, investors, and other stakeholders who need to understand a wind project's expected output and profitability before deciding on its development and operation. Several methods are available for wind resource assessment, including on-site measurements with meteorological towers and remote sensing tools like SODAR [4,5] (Sound Detection and Ranging) and LiDAR (Light Detection and Ranging) [6]. Additionally, numerical modeling and analysis of historical weather data are used as well. The outcomes of these assessments help determine the best operational design for wind turbine generators, enabling accurate predictions of energy production and the economic feasibility of the wind energy project [7].

Several researchers evaluated the wind resources in São João do Cariri, Paraíba state, in northeastern Brazil, from 2006 to 2009. Measurements of wind speed, wind direction, and air temperature were taken at heights of 25 m and 50 m, using 10-minute data recorded by the SONDA (Sistema Nacional de Organização de Dados Ambientais) meteorological station. The Weibull shape and scale factors were calculated with the WAsP program. The cost of generating energy from wind was found to be €0.046/kWh at 25 m height, using a 300 kW rated turbine with a capacity factor of 14.5% [8]. The turbine selection was based on three different types from the WAsP database, using the highest capacity factor and equivalent hours, a parameter employed to measure wind farm utilization. However, the wind turbine generator classification was not taken into account in this study.

Another study was conducted to assess wind resources in two municipalities, Paracuru and Triunfo, in Brazil's Northeast Region. Ten-minute wind data were gathered from anemometer towers and through simulations using the mesoscale Weather Research and Forecasting (WRF) model. This method was chosen to address the high costs and limited number of anemometer towers, leading to increased reliance on microscale and mesoscale numerical models. The WAsP model was used to estimate annual wind potential and power density based on both measured and simulated data. It was found that both locations have a favorable annual wind potential for developing wind farm projects. According to their assessments, the wind power density exceeded 400 W/m^2 at heights of 50 m and 60 m above ground level [9]. Once again, the classification of the wind turbine generator to be used and even the characteristic wind turbulence at the site were ignored.

Although Brazil does not yet have an offshore wind power plant, several studies on the regulatory framework, wind power potential, and economic analysis for developing offshore wind energy have already been conducted. Gonzalez et al. proposed a framework involving three main phases: Pre-development, Development and Operation, and Post-Operation. The framework suggests a feed-in tariff contracted in the tender, with readjustments based on the General Index of Market Prices. The research also concludes that the legal framework should consider the entire lifecycle of a wind farm, including decommissioning, to prevent regulatory issues [10]. Vinhoza and Schaeffer carried out an offshore wind energy potential assessment at various levels, including Gross, Technical, Environmental, and Social. They highlighted the most economically attractive areas for offshore wind deployment using Spatial Multi-Criteria Decision Analysis. Research results show that the least economically attractive areas are mainly in the Southeast region, while the most appealing ones are concentrated in the Northeast region [11]. Similarly, Lozer dos Reis et al. conducted an economic analysis of an offshore wind farm off the Brazilian coast using capital expenditures (CAPEX) and levelized cost of energy (LCOE) metrics, highlighting the preferred regions from both economic and energy perspectives. Research outcomes indicate that the Northeast region of Brazil, especially between Maranhão and Rio Grande do Norte, has a lower LCOE of US$69.90/MWh and CAPEX of US$2.34/MWh. Other less promising but still viable sites for offshore wind farm deployment include areas between northern Rio de Janeiro and southern Espírito Santo, as well as near Santa Catarina and Rio Grande do Sul [12]. Figure 3 shows the map of Brazil taken from Google Earth on 28 June 2025. Figure 4 illustrates the locations between Santa Catarina and Rio Grande do Sul in southeastern Brazil, taken from Google Earth on 20 July 2025.

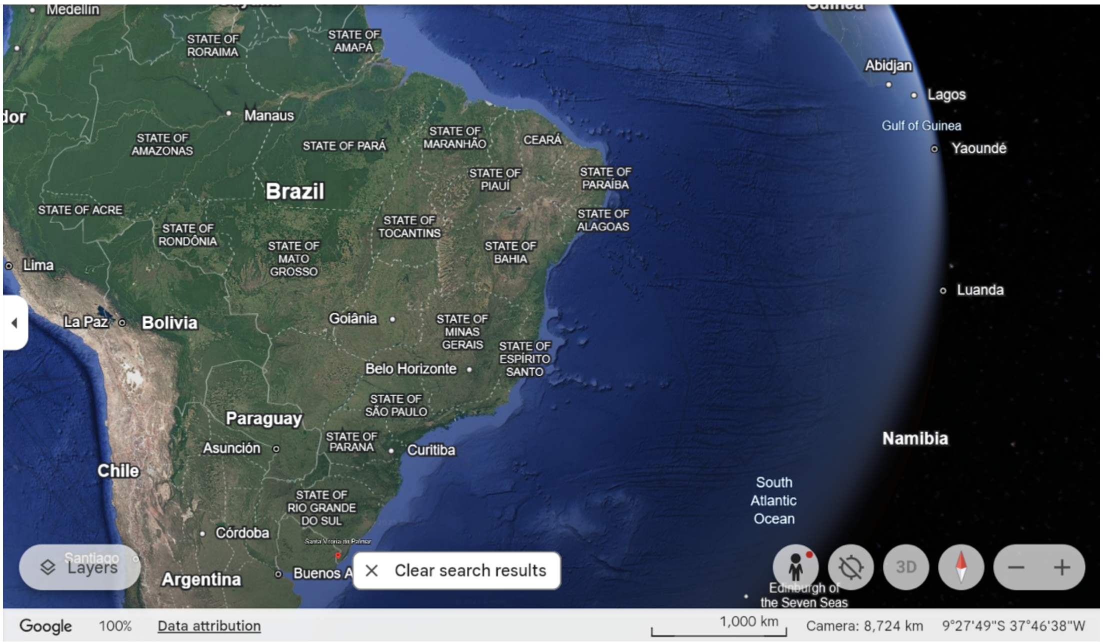

Figure 3. The map of Brazil was obtained from Google Earth (captured on 28 June 2025).

Figure 4. Viable site locations between State of Santa Catarina and State of Rio Grande do Sul taken from Google Maps (captured on 20 July 2025).

This study aims to better understand the wind energy potential in Rio Grande do Sul by conducting a wind resource assessment. The goal is to identify suitable onshore wind turbine sites for Phases I and II of the wind farms in Santa Vitoria do Palmar, which is the southernmost municipality of Brazil. This study explains how to determine Weibull parameters using various statistical estimation models and WAsP, select the appropriate turbine for the site that complies with IEC 61400-1 Edition 3 standards based on annual average wind speed and characteristic wind turbulence [13], estimate the annual energy yield and mean wind power density at hub height, and calculate the capacity factor, and levelized cost of energy for turbine selection. The final step involves using WAsP to numerically predict the wind farms' net annual energy production, considering the wake loss effects caused by terrain and turbine layout in the modeling.

2. Materials and Methodology

The layout for Phases I and II wind farms in Santa Vitoria do Palmar, Rio Grande do Sul, Brazil, is shown in Figure 5. The site is located at the southern tip of the country, bordering Argentina and Uruguay. Phases I and II require installing twelve (12) and fifty-five (55) land-based wind turbine generators, respectively. Figure 6 shows the coordinates of the meteorological mast in red, positioned at 33°34′12″ S latitude and 53°16′12″ W longitude, using Franson CoordTrans v2.3 software. Thies Clima Classic cup anemometers were installed at three heights on an anemometer tower: 60 m, 98 m, and 101 m above ground level. Table 1 provides details about the meteorological mast station, the instruments used, and the measurement period. Wind data collected included wind speed, standard deviation, wind direction, relative humidity, ambient temperature, and environmental pressure at 10-minute intervals from November 2006 to April 2008, complying with IEC 61400-12-1 Ed. 2005 standards for at least one year [14]. However, the data from the period between 1 April 2007, and 31 March 2008, were used for the wind resource analysis.

Table 1. Information on the meteorological mast, instrument, and measurement period.

Description	Value
Site Location	Santa Vitoria do Palmar, State of Rio Grande do Sul, Brazil
Mast Coordinates	33.57° S Latitude and 53.27° W Longitude
Instrument	Cup Anemometer Type Thies Clima Classic
Sensor Height (a.g.l.)	60 m, 98 m, and 101 m
Measurement Period	1 November 2006–9 April 2008

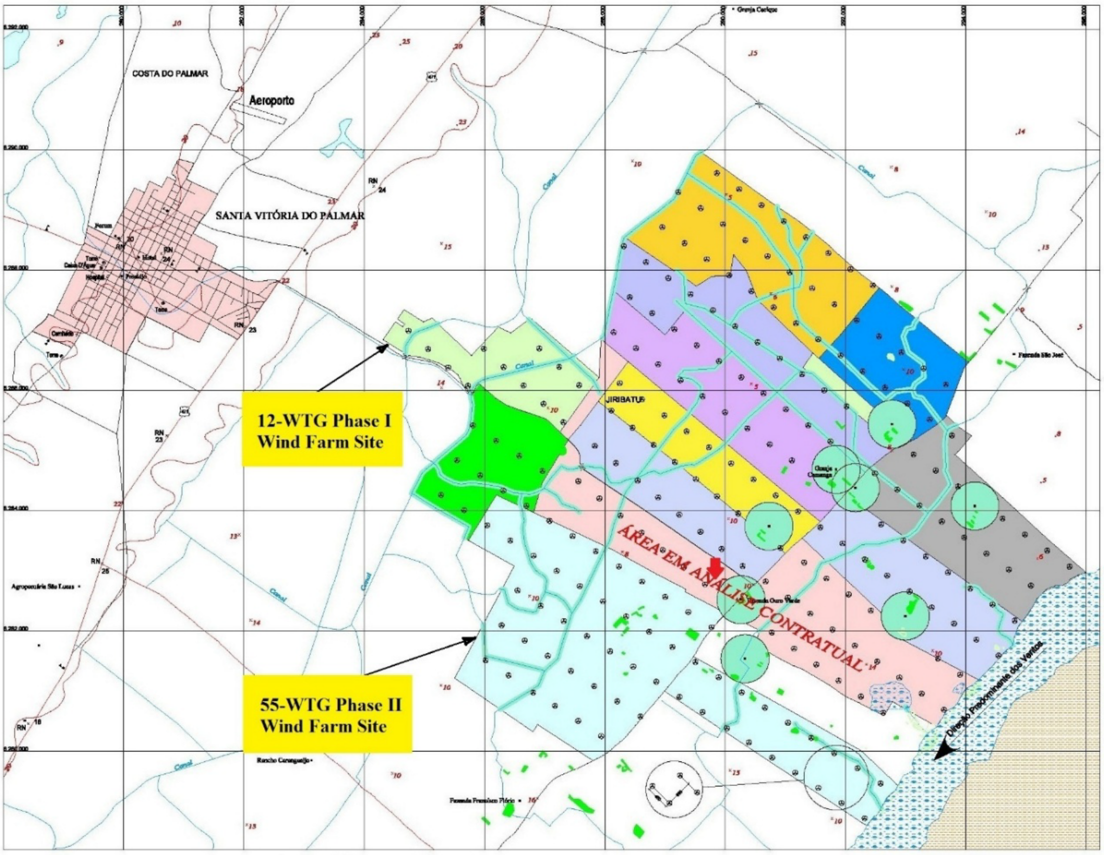

Figure 5. Site layouts for Phases I and II wind farms in SVdP, Brazil.

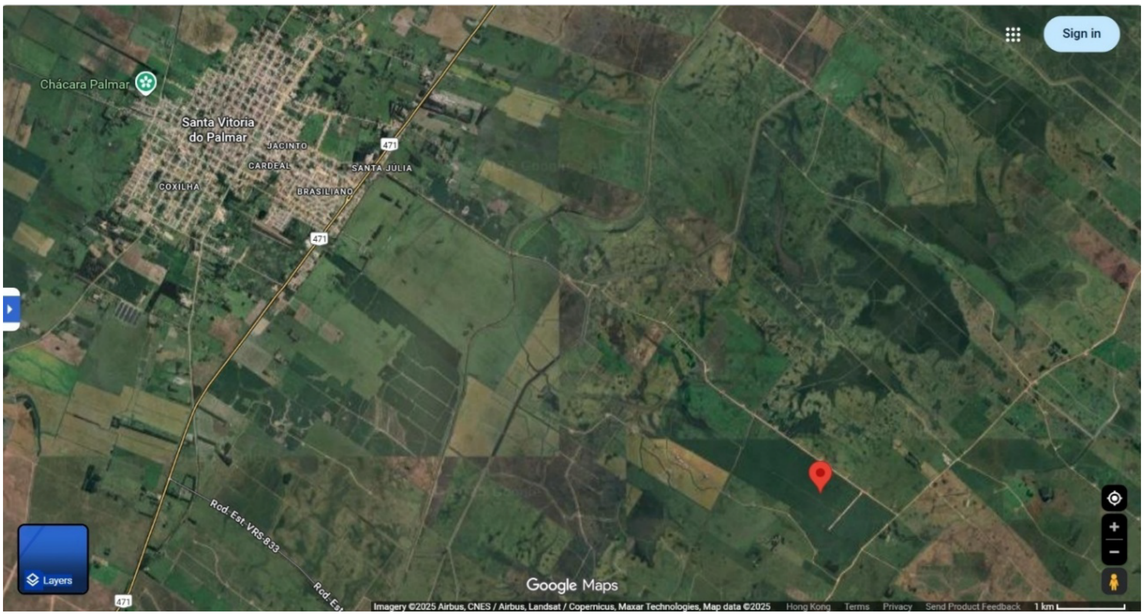

Figure 6. Meteorological mast location in SVdP in the State of Rio Grande do Sul, Brazil.

2.1. Research Design

The wind resource assessment was performed to determine the energy potential from the wind at the site. This process typically involves collecting and analyzing 10-minute meteorological data over at least one year, including wind speed, standard deviation, relative humidity, wind direction, ambient temperature, and environmental pressure, all of which can influence wind power generation and must comply with IEC 61400-12-1 guidelines. Key metrics to be calculated include the Weibull parameters, wind shear exponent, roughness factor, wind rose, wind frequency, and mean wind power density. The Weibull parameters can be estimated using various statistical models such as the graphical method, standard deviation method, maximum likelihood method, energy pattern factor method, and

Rayleigh distribution [15]. WAsP results will also be used and compared with these statistical estimation models. Once the Weibull parameters are known, the annual average wind speed, probability density function (PDF), and cumulative distribution function (CDF) can be derived. Knowing the annual average wind speed and the characteristic wind turbulence—based on turbulence intensity and standard deviation—helps determine the suitability of wind turbine generators for the site. Additionally, multiplying the turbine power curve by the probability density function can estimate the annual energy yield at hub height. The selection of turbines was based on achieving the maximum capacity factor while keeping the levelized cost of energy (LCOE) low. This approach ensures a thorough and accurate process for selecting turbines, and the computations were done using Visual Basic and user-defined functions in the Macro platform of MS Excel. The final step involved using WAsP to numerically predict the wind farm's net annual energy production, considering wake loss effects due to terrain and turbine arrangement. Figure 7 illustrates the methodological flow of the study.

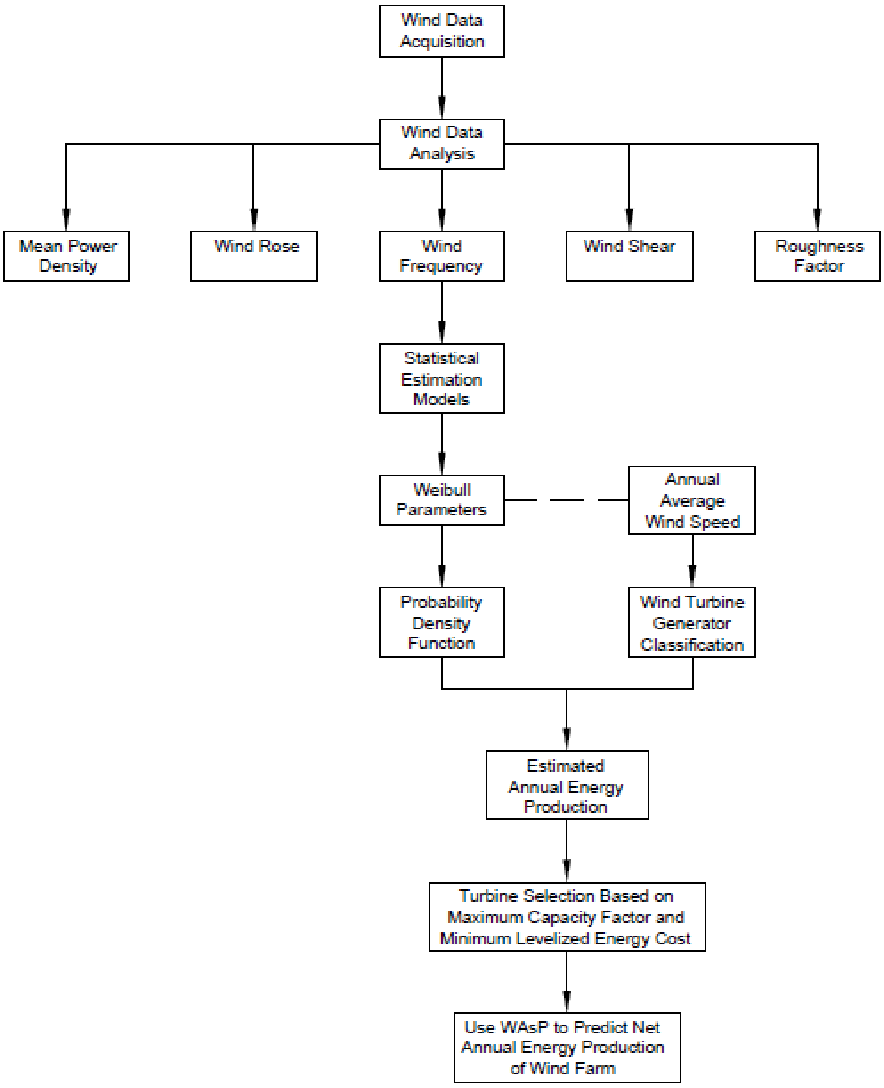

Figure 7. A flow chart showing the methodological flow of the study.

2.2. Monthly Mean Wind Speed and Wind Shear Profiles

The mean wind speed, denoted as V_m, was calculated using Equation (1) as shown below

$$V_m = \frac{1}{N}\sum_{i=1}^{N} V_i \tag{1}$$

where the measured time-mean wind speed value is denoted by V_i and N represents the number of data points. A calm threshold of 0.3 m/s was used. Readings below 0.3 m/s were set to zero. The wind shear coefficient was calculated as follows [16,17]:

$$\alpha = \frac{\ln V_b - \ln V_a}{\ln z_b - \ln z_a} \tag{2}$$

where V_b and V_a are wind speeds measured at their corresponding heights of z_b =101 m and z_a =60 m.

2.3. Statistical Estimation Methods

In this study, various analytical estimation models were used to determine the Weibull parameters, including the graphical method (GM), standard deviation method (SD), energy pattern factor method (EPF), maximum likelihood method (MM), and Rayleigh distribution (RD). Due to the intermittent or stochastic nature of wind, the Weibull parameters were applied to calculate the cumulative distribution and probability density functions of wind conditions. *f(V)* is known as the probability density function, which refers to the fraction of time during which wind is present at a given velocity. It can be written as

$$f(V) = \frac{k}{A^k} V^{(k-1)} \exp\left[-\left(\frac{V}{A}\right)^k\right] \tag{3}$$

Meanwhile, the cumulative distribution function denoted as *F(V)* is used to describe the fraction of time or probability that the measured wind speed is less than or equal to the given velocity *V*. It can be obtained by summing up the probability density function in the form of

$$F(V) = 1 - \exp\left[-\left(\frac{V}{A}\right)^k\right] \tag{4}$$

2.3.1. Graphical Method

The cumulative distribution profile in the graphical method transforms into a linear form using logarithmic scales, wherein Equation (4) becomes

$$1 - F(V) = \exp\left[-\left(\frac{V}{A}\right)^k\right] \tag{5}$$

Applying the natural logarithm twice,

$$\ln\{-\ln(1 - F(V))\} = k \ln\left(\frac{V}{A}\right) \tag{6}$$

Equation (6) turns into a general equation of a line in a logarithmic scale with the slope as the shape factor. The scale factor can be identified using Equation (7), where $\hat{b}$ is the absolute value of the *y*-intercept.

$$A = \exp\left[\frac{\hat{b}}{k}\right] \tag{7}$$

2.3.2. Standard Deviation Method

The standard deviation method estimates the Weibull parameters using wind speed and standard deviation sampling data. The allowable approximation for the shape factor [18] is given by

$$k = \left(\frac{\sigma}{V_m}\right)^{-1.09} \tag{8}$$

where σ represents the standard deviation, which can be computed by the following formula [19]:

$$\boldsymbol{\sigma} = \sqrt{\frac{\mathbf{1}}{\boldsymbol{N} - \mathbf{1}} \sum_{\boldsymbol{i}=\mathbf{1}}^{\boldsymbol{N}} (\boldsymbol{V_i} - \boldsymbol{V_m})^{\mathbf{2}}} \tag{9}$$

For more accurate scale factor results, the following expression can be used [20].

$$A = \frac{V_m k^{2.6674}}{0.184 + 0.816 k^{2.73855}} \tag{10}$$

2.3.3. Energy Pattern Factor Method

A less computational approach that estimates the ratio of available wind power potential to the power proportionate to the cube of the average wind speed is known as the energy pattern factor method [21].

$$E_{PF} = \frac{\frac{1}{N}\sum_{i=1}^{N} V_i^3}{\left(\frac{1}{N}\sum_{i=1}^{N} V_i\right)^3} \tag{11}$$

Knowing the E_{PF} from wind data, the predicted shape factor can be determined using Equation (12).

$$k = 3.957 E_{PF}^{-0.898} \tag{12}$$

On the other hand, the scale factor can be obtained using the measured annual mean wind speed and the Gamma function, as shown below.

$$A = \frac{V_m}{\Gamma\left(1 + \frac{1}{k}\right)} \tag{13}$$

2.3.4. Maximum Likelihood Method

In the maximum likelihood method, the shape factor is given as shown in Equation (14)

$$k = \left[\frac{\sum_{i=1}^{n} V_i^k \ln(V_i)}{\sum_{i=1}^{n} V_i^k} - \frac{\sum_{i=1}^{n} \ln(V_i)}{n}\right]^{-1} \tag{14}$$

where the k value was determined using root-finding method such as fixed-point iteration. The scale factor was computed using the following formula [22,23].

$$A = \left[\frac{1}{n}\sum_{i=1}^{n} V_i^k\right]^{1/k} \tag{15}$$

2.3.5. Rayleigh Distribution

In the Rayleigh distribution, the Weibull parameters can be predicted with a shape factor set equal to 2, and the scale factor can be calculated using Equation (16).

$$A = \frac{2V_m}{\sqrt{\pi}} \tag{16}$$

2.4. Wind Atlas Analysis and Application Program (WAsP)

One of the tools for assessing wind resources is the WAsP software (DTU Wind and Energy Systems, Roskilde, Denmark), which numerically calculates and tabulates various parameters, including Weibull parameters, frequency distribution tables, probability density functions, wind roses, annual mean wind speed, and mean power density. WAsP is specifically designed for wind resource assessment and wind turbine siting. It analyzes wind data to forecast wind climates, resources, and the energy outputs of turbines. Additionally, the software estimates wind power potential and evaluates how obstacles and terrain impact wind flow.

3. Results and Discussion

3.1. Mean Wind Speed and Wind Shear Profiles at Reference Heights

The monthly average wind speeds at heights of 60 m, 98 m, and 101 m are shown in Figure 8. The highest average wind speed of 9.30 m/s was recorded at a sensor height of 101 m in August 2007. Additionally, the annual average wind speeds at these sensor heights are 7.70 m/s, 8.18 m/s, and 8.32 m/s, respectively.

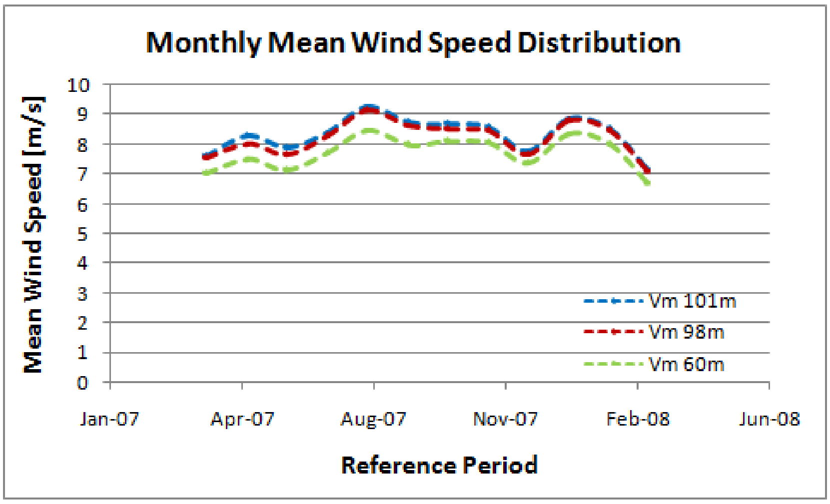

Figure 8. Mean wind speed profile at different sensor heights from April 2007 to March 2008.

Values of the wind shear coefficient at two sensor heights of 60 m and 101 m were calculated sector-wise, as shown in Figure 9. Figure 10 also shows the monthly mean wind shear distribution.

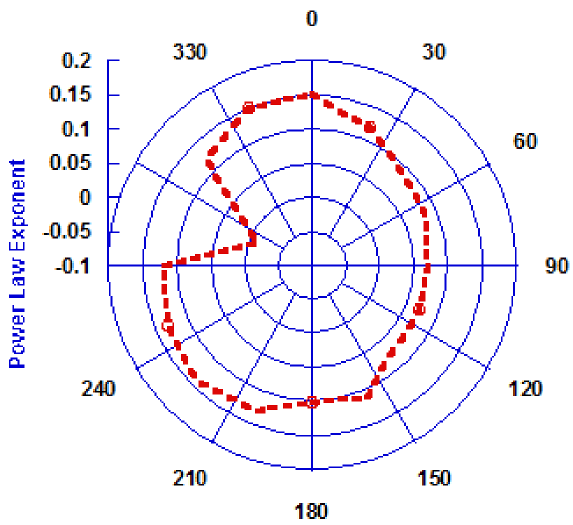

Figure 9. Wind shear coefficient profile arranged sector-wise.

The annual average wind shear coefficient was 0.11, with an overall roughness length of 0.01 m, indicating that the terrain is typical of open country with little to no significant structures or vegetation.

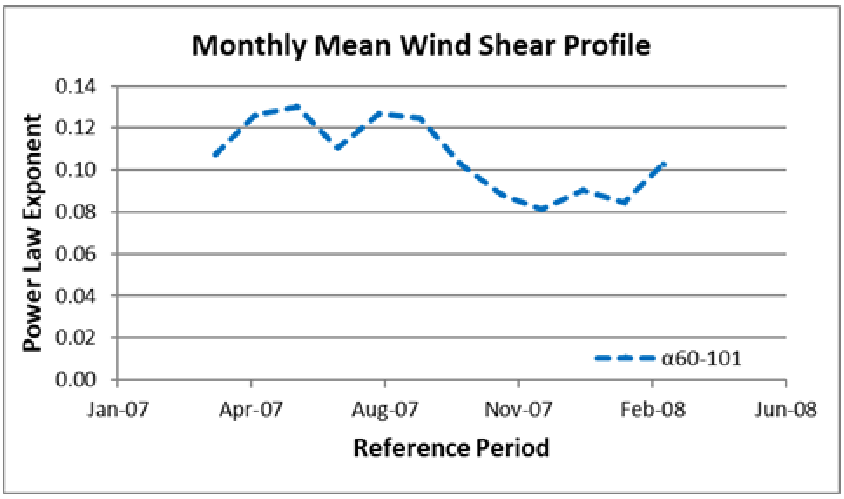

Figure 10. Monthly mean wind shear profile from April 2007 until March 2008.

3.2. Identification of Weibull Parameters

Figure 11a,b illustrate how the cumulative distribution function is converted into a linear form using logarithmic scales through the graphical method at reference and hub heights of 101 m and 80 m, respectively. The wind speeds at 80 m were interpolated using Equation (2). The correlation coefficient in linear form for both figures exceeds 99%.

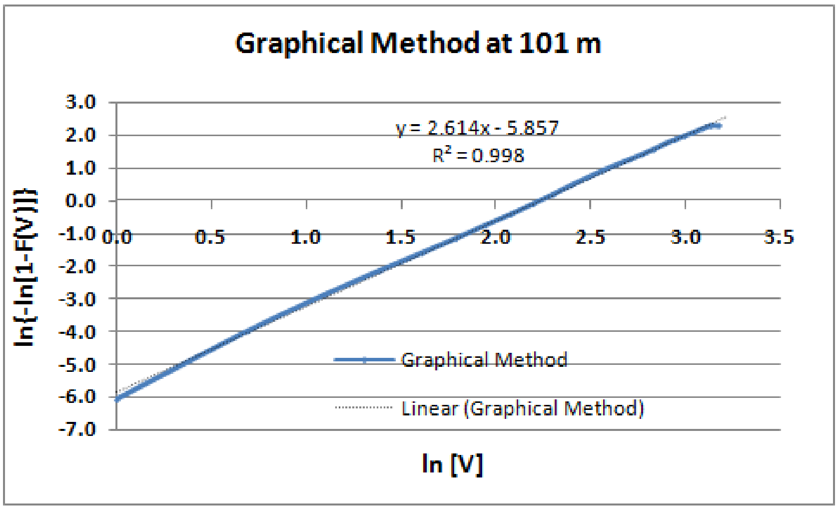

(**a**)

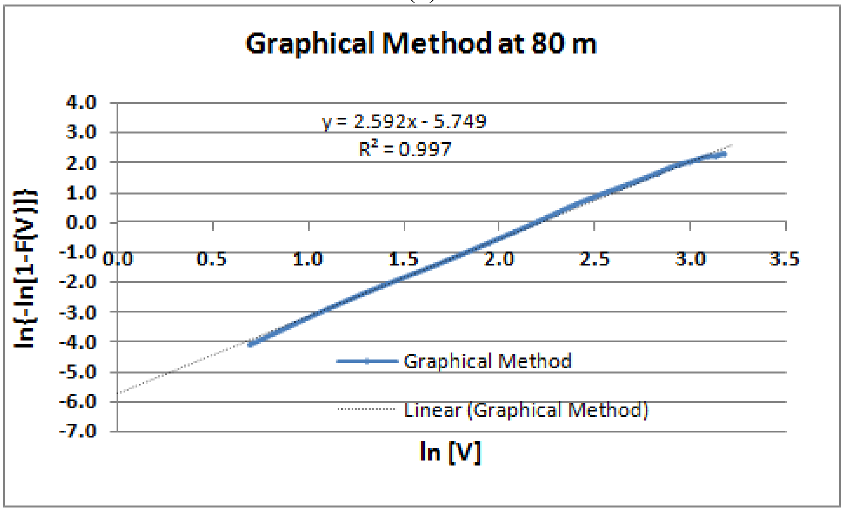

(**b**)

Figure 11. Weibull parameters using graphical method at the heights of (**a**) 101 m and (**b**) 80 m.

Equations (6)–(16) were used to calculate the shape and scale factors for different statistical estimation models. Table 2 summarizes the Weibull parameters obtained from these models and WAsP numerical output at a reference height of 101 m and a hub height of 80 m. The analysis shows that the Weibull parameters from the energy pattern factor model are more comparable to those produced by WAsP.

Table 2. Weibull parameters using various statistical estimation models and WAsP at 101 m and 80 m.

Elevation	Weibull Parameters	GM	SD	RD	EPF	MLM	WAsP
101 m	Shape Factor, *k*	2.61	2.66	2.00	2.72	2.64	2.72
	Scale Factor, *A* [m/s]	9.40	9.37	9.39	9.41	9.36	9.40
80 m	Shape Factor, *k*	2.59	2.70	2.00	2.74	2.68	2.73
	Scale Factor, *A* [m/s]	9.19	9.03	9.06	9.06	9.03	9.10

Figure 12 shows the wind rose and frequency distribution created from the OWC wizard from WAsP at a 101 m reference height. Kaleidagraph software (Synergy Software, Reading, PA, USA) was also used to plot data for comparison to identify the wind frequency rose. Both figures show that the most common wind came from 30° E of N, with the highest wind speeds throughout August 2007.

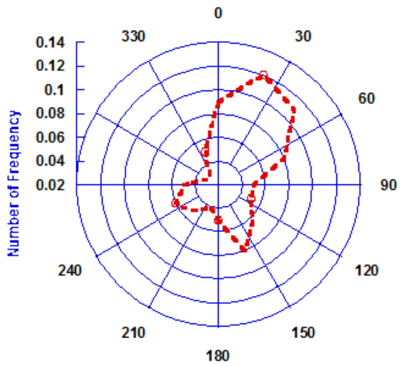

(**a**)

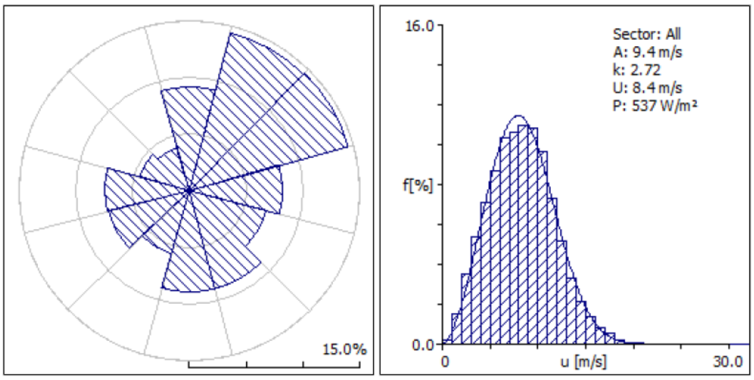

(**b**)

Figure 12. Wind rose and probability density function using (**a**) Kaleidagraph and (**b**) WAsP at 101 m.

Figure 13 shows the numerical results from WAsP at an 80 m hub height, including the wind rose, probability density function profile with a shape factor of 2.73, scale factor of 9.10 m/s, an annual average wind speed of 8.10 m/s, and a mean wind power density of 478 W/m^2.

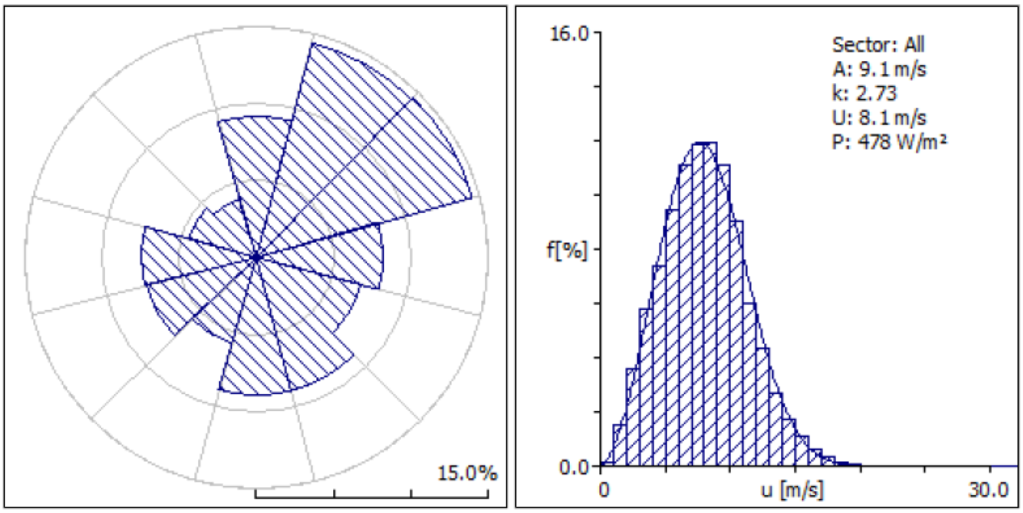

Figure 13. Wind rose and Weibull parameters using WAsP at 80 m hub height.

To identify which statistical estimation model most closely resembles WAsP, we plotted the probability density function (PDF) at a reference height of 101 m and at a hub height of 80 m for comparison. These plots are shown in Figure 14a,b. The correlation coefficients between the statistical estimation models and WAsP, calculated using Student's *t*-test, were compared as shown in Table 3, with twenty-five (25) degrees of freedom. Since the computed *t*-value is less than the critical t-value, the correlated samples are considered the same with a confidence level above 97.5%. The results indicate that the energy pattern factor method is preferred, with a PDF correlation coefficient of 100%.

Table 3. PDF Student's *t*-Test between statistical estimation models and WAsP at 101 m and 80 m.

Elevation	Description	GM vs. WAsP	SD vs. WAsP	MLM vs. WAsP	EPF vs. WAsP
101 m	*t*-value	0.006	0.006	0.115	0.001
	t-probability	0.995	0.996	0.910	0.999
	Correlation	99.94%	99.97%	99.94%	100%
	c-value	2.06	2.06	2.06	2.06
80 m	*t*-value	0.006	0.003	0.278	0.002
	t-probability	0.995	0.998	0.783	0.999
	Correlation	99.90%	99.98%	99.95%	100%
	c-value	2.06	2.06	2.06	2.06

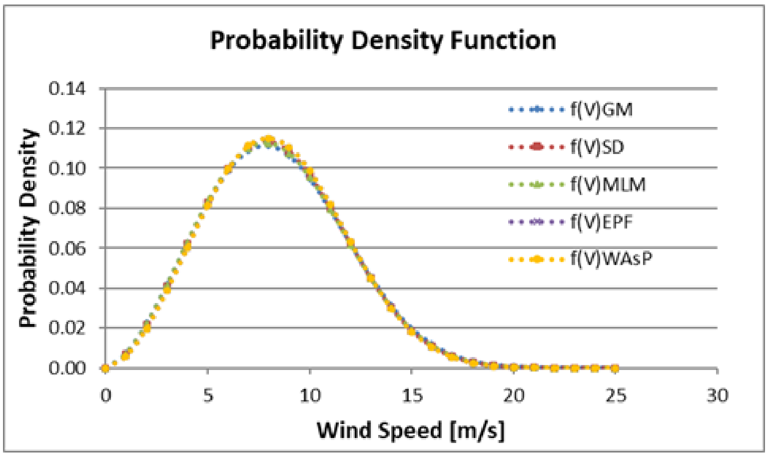

(**a**)

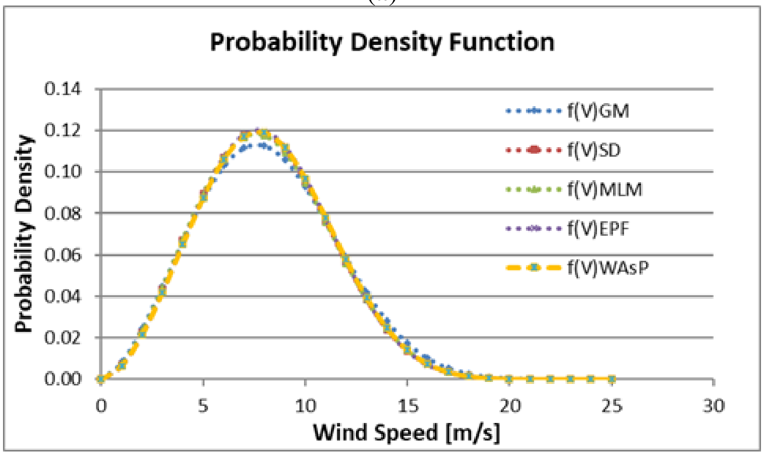

(**b**)

Figure 14. Probability density functions at the (**a**) reference height of 101 m and (**b**) hub height of 80 m.

3.3. Annual Average Wind Speed at Reference and Hub Heights

The measured annual average wind speed was also compared with the WAsP Weibull-fit value at different sensor heights on the meteorological mast station. The percentage discrepancy was calculated using Equation (17). The results are summarized in Table 4, with values less than 1.1%.

$$\%\,Error = \left|\frac{V_{Weibull-fit} - V_{measured}}{V_{Weibull-fit}}\right| \times 100\% \quad (17)$$

Table 4. Annual mean wind speed at various sensor heights of meteorological mast station and at 80 m.

Description	**Reference Height**			**Hub Height**
	101 m	**98 m**	**60 m**	**80 m**
$V_{measured}$ using Equation (1)	8.32 m/s	8.18 m/s	7.70 m/s	8.03 m/s
$V_{WAsP\ Weibull\text{-}fit}$ using G function	8.36 m/s	8.27 m/s	7.74 m/s	8.10 m/s
Percent Error	0.48%	1.08%	0.49%	0.82%

The measured and WAsP Weibull-fit values of annual average wind speed at 80 m hub height were calculated using Equation (1) and the gamma function, respectively, as shown in Table 4, with a discrepancy of 0.82%. Results indicate that the annual mean wind speed at hub height is 8.10 m/s, suggesting that the site is suitable for an IEC Class II wind turbine generator [13].

3.4. Wind Power Density

The mean wind power density, denoted as W_{PD} measures the available wind energy per turbine's swept area, which is mathematically described as

$$W_{PD} = \frac{1}{2N}\sum_{i=1}^{N}\rho_i V_i^3 \quad (18)$$

where ρ_i and V_i are the 10-minute time-mean air mass density and wind speed, respectively. The air mass density was computed in terms of ambient temperature T [K], relative humidity ϕ, and barometric pressure B [Pa] using the following equations obtained from the IEC 61400-12-1 guidelines.

$$\rho = \frac{1}{T}\left[\frac{B}{R_0} - \emptyset P_w\left(\frac{1}{R_0} - \frac{1}{R_w}\right)\right] \quad (19)$$

The R_0, R_w, and P_w denote the dry air gas constant [287.05 J/kg-K], the water vapor gas constant [461.5 J/kg-K], and vapor pressure [Pa], respectively. The vapor pressure depends on the mean air temperature as shown below.

$$P_w = 0.0000205 \exp(0.0631846T) \quad (20)$$

Table 5 shows the average wind power density at three different sensor heights on the meteorological mast station in SVdP, Brazil, along with a hub height of 80 m. The table also provides the average wind power density from WAsP for comparison. The results indicate that the errors were less than 6.40%. The difference is due to the air mass density value used in WAsP, which is 1.225 kg/m^3, compared to the site's actual average air mass density of 1.150 kg/m^3 over one year.

Table 5. Wind power density at various sensor heights of meteorological mast and hub height of 80 m.

Description	Reference Height			Hub Height
	101 m	98 m	60 m	80 m
W_{PD} using Equation (16)	502.72 W/m^2	476.62 W/m^2	391.80 W/m^2	447.54 W/m^2
W_{PD} from WAsP	537.00 W/m^2	509.00 W/m^2	418.00 W/m^2	478.00 W/m^2
Percent Error	6.38%	6.36%	6.27%	6.37%

The wind power density at 50 m (a.g.l.) was 368.53 W/m^2 for one year. The wind energy generation classification from the National Renewable Energy Laboratory indicates that at a reference height of 50 m (a.g.l.), the site resource is moderate, corresponding to wind class 3. The acceptable wind speed range is between 6.2 m/s and 6.9 m/s, with the wind power density ranging from 300 to 400 W/m^2 as shown in Table 6 [24,25].

Table 6. Classification of wind energy generation at 50 m (a.g.l.) from NREL.

Wind Class	Resource	Wind Speed [m/s]	Wind Power Density [W/m^2]
1	Poor	0.0–5.4	0–200
2	Marginal	5.4–6.2	200–300
3	Moderate	6.2–6.9	300–400
4	Good	6.9–7.4	400–500
5	Excellent	7.4–7.8	500–600
6	Excellent	7.8–8.6	600–800
7	Excellent	>8.6	>800

3.5. Turbulence Characteristics

The turbulence properties were determined using wind speed and standard deviation data for each speed bin over a 10-minute interval at a reference height of 101 m. The turbulence characteristics can be estimated following the guidelines in Section 6.3.1.3 of IEC 61400-1 Edition 3, which include Figure 15a,b for predicting wind turbulence based on standard deviation and turbulence intensity.

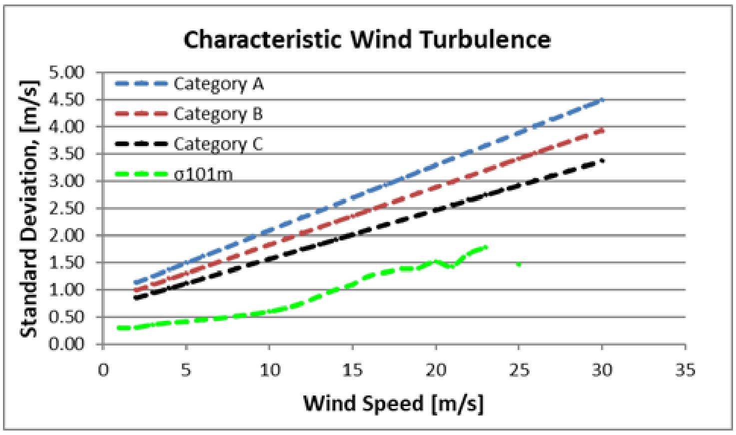

(a)

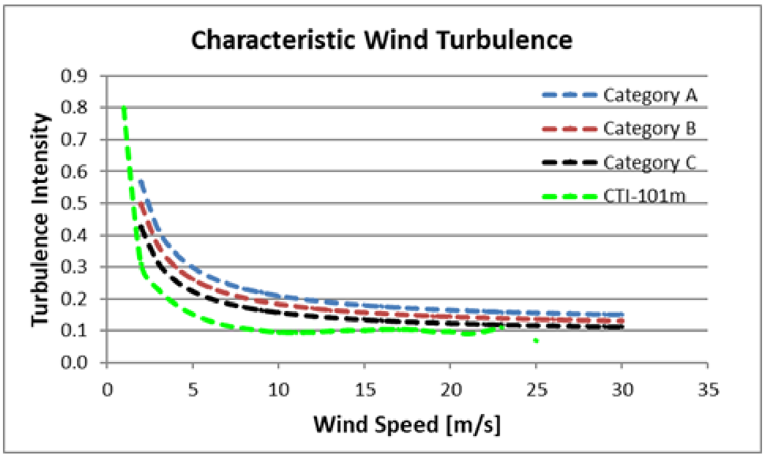

(**b**)

Figure 15. Characteristic wind turbulence based on (**a**) standard deviation; and (**b**) turbulence intensity.

The blue, red, and black colors in the figures above represent the upper, middle, and lower bounds of turbulence intensity, also known as Categories A, B, and C, respectively. The green color indicates the characteristic wind turbulence at 101 m using the calculation results shown in both figures. The wind turbulence at the site appears to be below Category C, suggesting that the area is suitable for IEC Subclass C. To verify our analytical calculations, Windographer software (UL Solutions, Aiken, SC, USA) was also used to determine the characteristic wind turbulence based on turbulent intensity, as shown in Figure 16. Figures 15b and 16 display similar results.

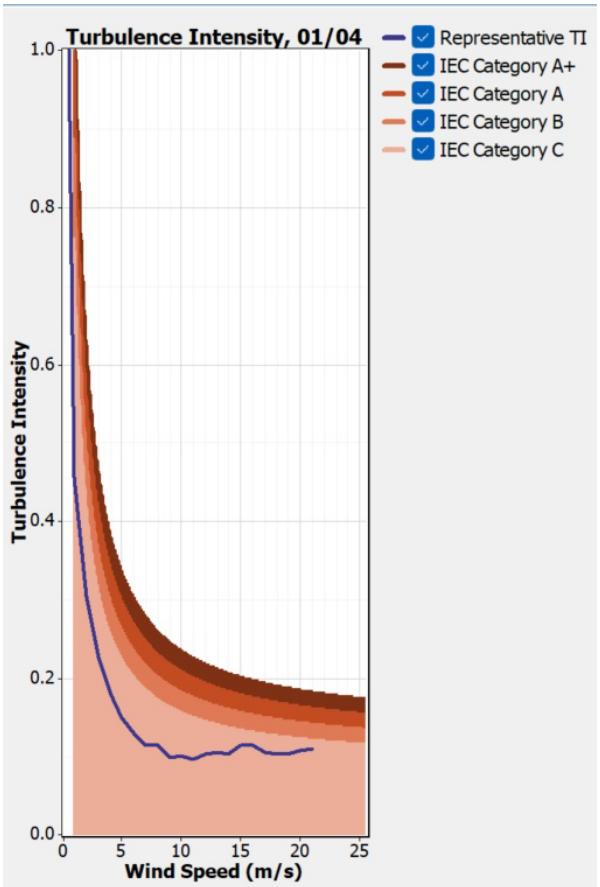

Figure 16. Characteristic wind turbulence based on turbulence intensity at 101 m using Windographer.

3.6. Estimated Annual Energy Production

The estimated annual energy production (*AEP*) is determined by the product of the probability density function at hub height and the horizontal-axis wind turbine power curve, as per Equation (21). N_h stands for the number of hours per year, which is 8760 according to IEC 61400-12-1, while n refers to the number of speed bins with a step size of 0.1 m/s.

$$AEP = N_h \int_{cut-in}^{cut-out} P(V) f(V) dV \tag{21}$$

The above equation can be evaluated using numerical integration and can be rewritten as

$$AEP = N_h \sum_{i=1}^{n} \left[\frac{P_i f_i + P_{i-1} f_{i-1}}{2}\right] (V_i - V_{i-1}) \tag{22}$$

Based on the site requirements, the wind turbine generators must meet IEC Class II standards. After careful review, the following turbines have been selected: Enercon E-82, Vestas V90, Nordex N-90, NEG Micon NM92, and Avantis AV928. Table 7 provides key details for each turbine, including rated power, rotor diameter, swept area, presence of a gearbox, and hub height. This information is vital for determining the most suitable turbine for the site. Figure 17a,b illustrate the power curves for various wind turbine generators equipped with gearboxes and power curves for gearless wind turbines, respectively.

Table 7. Detailed information on different IEC Class II wind turbine generators.

Description	E-82	V90	N-90	NM92	AV928
Rated Power [MW]	2.35	3.00	2.30	2.75	2.50
Rotor Diameter [m]	82	90	90	92	93.2
Swept Area [m^2]	5281	6362	6362	6648	6822
Presence of gearbox	No	Yes	Yes	Yes	No
Hub Height [m]	80	80	80	80	80

Table 8 shows that the 2.5MW AV928 wind turbine generator has the highest capacity factor of 41.22% and predicted annual energy production of 9589.09 MWh/year, making it the best turbine for the site.

$$C_f = \frac{Annual\ Energy\ Production}{8760 \times Turbine\ Rated\ Power} \times 100\% \tag{23}$$

Table 8. Predicted annual energy production for different wind turbine generators.

Description	E-82	V90	N90	NM92	AV928
AEP [MWh/yr]	8588.57	9844.40	8856.37	9751.57	9589.09
Capacity Factor	38.93%	34.05%	39.96%	36.80%	41.22%

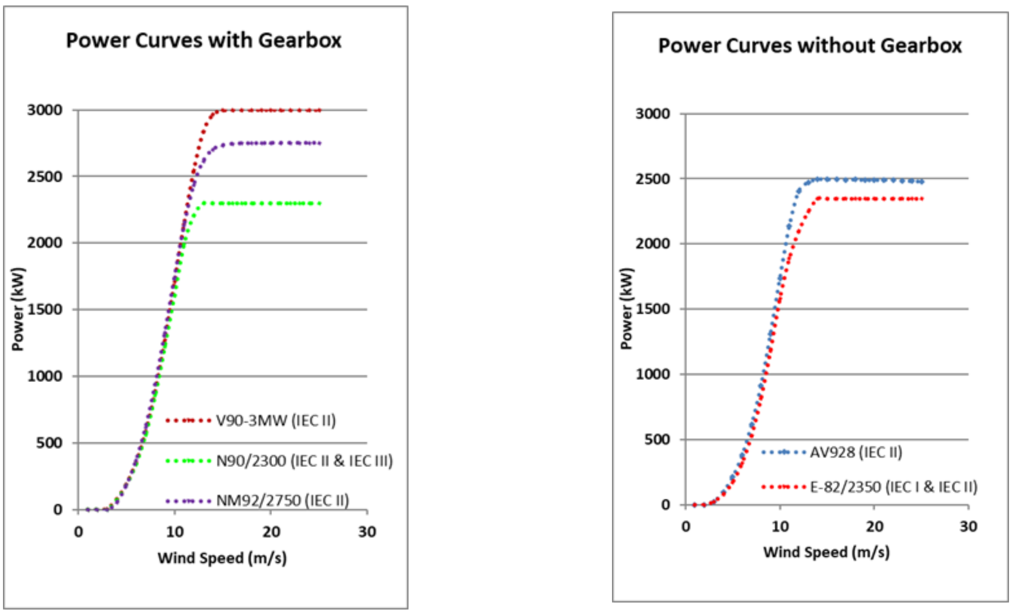

(**a**) (**b**)

Figure 17. Power curves of wind turbine generator (**a**) with gearbox; and (**b**) without gearbox.

3.7. Levelized Cost of Energy

This section aims to explain the cost of assessing energy generated from the available wind potential using various types of wind turbine generators with the same IEC Class II. The primary objective is to provide an understanding of the current component-level costs and a basis for comprehending the variation in wind energy based on the levelized cost of energy for land-based wind power plants. The levelized cost breakdown for reference land-based wind power plants is as follows: turbine capital expenditures, balance of system capital expenditures, soft costs, and operational expenditures, with percent distributions of 41%, 22%, 11%, and 26%, respectively [26]. The levelized cost of energy can be calculated using the following formula:

$$LCOE = \frac{[C_{CapEx} \times FCR] + C_{OpEx}}{AEP_{Net}} \quad (24)$$

where C_{CapEx}, C_{OpEx}, AEP_{Net}, and FCR represent the capital expenditures, operational expenditures, net annual energy production, and fixed charge rate, respectively. The net annual energy production is a product of the overall turbine efficiency and the estimated annual energy production.

Table 9 presents the economic evaluation of different wind turbine generators. The findings show that the 2.5MW AV928 wind turbine generator has the lowest levelized cost of energy at US$44.36/MWh.

Table 9. Summary of economic assessment using various types of wind turbines.

Description	E-82	V90	N90	NM92	AV928
Wind Turbine Rating [MW]	2.35	3.00	2.30	2.75	2.50
Capital Expenditures [$1750/kW]	4,112,500	5,250,000	4,025,000	4,812,500	4,375,000
Fixed Charge Rate [%/yr]	6.73%	6.73%	6.73%	6.73%	6.73%
Operational Expenditures[$41/kW/yr]	96,350	123,000	94,300	112,750	102,500
Net AEP [MWh/yr]	8014.00	8949.46	8051.25	8865.06	8947.58
Levelized Cost of Energy [$/MWh]	$46.56	$53.22	$45.36	$49.25	$44.36

3.8. Net Annual Energy Production of Wind Farms using WAsP

Among the wind turbine generators mentioned above, the 2.5MW AV928 has a maximum capacity factor of 41.22% but the lowest levelized energy cost of US$44.36/MWh, making it one of the most efficient and promising options for wind power generation at the site. To assess its performance, a power curve, a contour map with roughness, and 10-minute wind data collected over a year were input into WAsP. This produced a local wind climate report detailing wind distributions for various surface roughness parameters and elevations ranging from 10 m to 200 m, as listed in Table 10. Since surface roughness is not present in the vector map, the site is assumed to be flat land with a roughness factor of 0.03 m. For Phase I, twelve units of AV928 wind turbine generators would be needed, and for Phase II, fifty-five units, with a total capacity of 30 MW and 137.5 MW, respectively. Please refer to Figure 18 for more details.

WAsP provided a detailed breakdown of the gross and net annual energy production for the proposed wind farms. The net annual energy yields for Phase I and Phase II wind farms, considering the wake loss effect, were found to be 104.92 GWh and 456.89 GWh, respectively. Further details of the results can be found in Table 11.

Table 10. WAsP regional wind climate summary in SVdP in the State of Rio Grande do Sul, Brazil.

Elevation	Description	0.00 m	0.03 m	0.10 m	0.40 m
10 m	Weibull scale factor [m/s]	8.34	5.76	5.05	3.98
	Weibull shape factor	2.57	2.18	2.17	2.15
	Mean wind speed [m/s]	7.38	5.11	4.45	3.51
	Wind power density [W/m^2]	385	145	96	48
25 m	Weibull scale factor [m/s]	9.06	6.85	6.16	5.19
	Weibull shape factor	2.64	2.34	2.31	2.28
	Mean wind speed [m/s]	8.08	6.10	5.48	4.62
	Wind power density [W/m^2]	495	233	170	103
50 m	Weibull scale factor [m/s]	9.75	7.93	7.24	6.27
	Weibull shape factor	2.71	2.60	2.54	2.46
	Mean wind speed [m/s]	8.67	7.03	6.40	5.56
	Wind power density [W/m^2]	601	331	254	170
100 m	Weibull scale factor [m/s]	10.54	9.33	8.54	7.55
	Weibull shape factor	2.63	2.78	2.78	2.78
	Mean wind speed [m/s]	9.38	8.29	7.60	6.70
	Wind power density [W/m^2]	775	519	399	273

Table 10. *Cont.*

Elevation	Description	0.00 m	0.03 m	0.10 m	0.40 m
200 m	Weibull scale factor [m/s]	11.64	11.51	10.44	9.15
	Weibull shape factor	2.51	2.68	2.68	2.69
	Mean wind speed [m/s]	10.33	10.22	9.31	8.14
	Wind power density [W/m^2]	1071	996	750	499

Table 11. Predicted annual energy yield with wake loss effects for Phases I and II wind farms.

Description	Phase I Wind Farm	Phase II Wind Farm
Gross annual energy yield [MWh]	110,686.09	508,055.62
Net annual energy yield [MWh]	104,915.27	456,891.53
Wake loss effect [%]	5.21%	10.07%

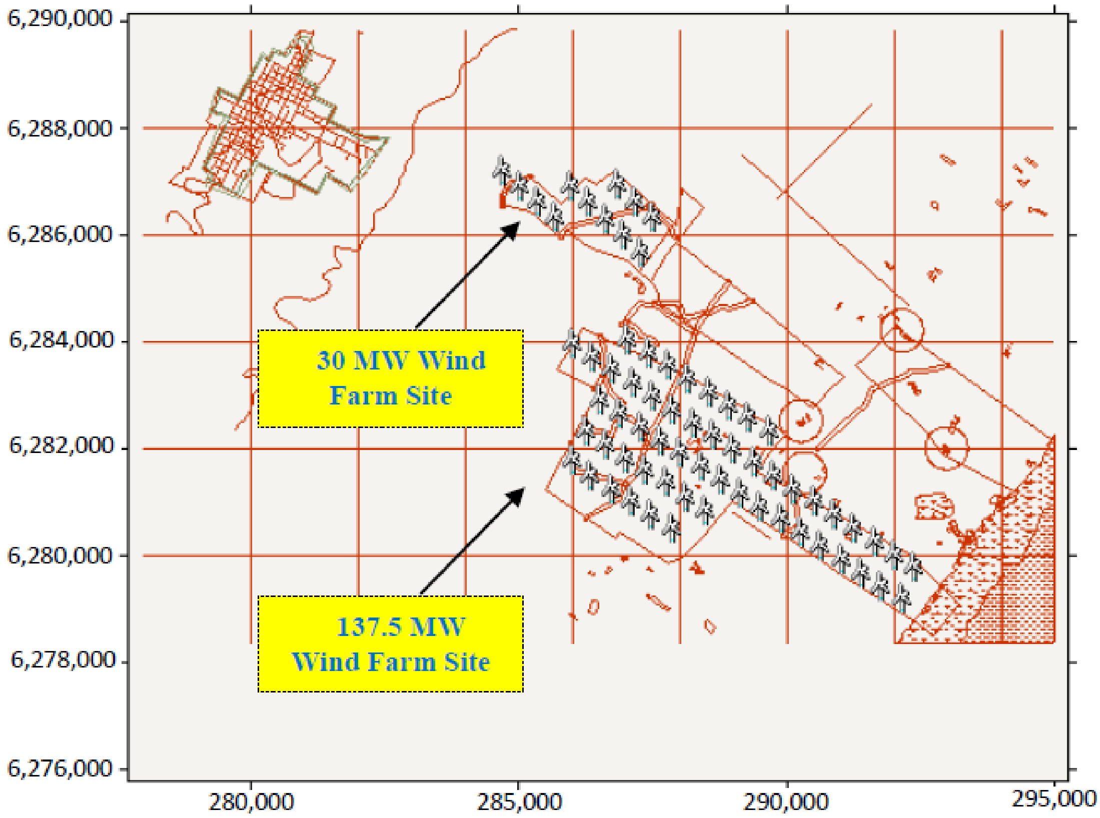

Figure 18. Turbine arrangements for Phases I and II wind farms in SVdP, Brazil.

The WAsP report examines the wind turbine cluster for two wind farms in SVdP, Brazil. Appendix A details the 30 MW Phase I wind farm, while Appendix B covers the 137.5 MW Phase II wind farm. The report outlines the turbine layouts, their coordinates, and annual energy production figures. The results emphasize the impact of wake loss on individual turbines.

4. Conclusions

A preliminary study of wind resource assessment was carried out to determine the most suitable type of horizontal axis wind turbine generator for Phases I and II wind farms in Santa Vitoria do Palmar, in. the State of Rio Grande do Sul, Brazil. The assessment used wind data collected from 1 April 2007, to 31 March 2008, which included wind speed, standard deviation, wind direction, relative humidity, ambient temperature, and atmospheric pressure, all recorded at 10-minute intervals. Several analytical models were used to estimate the Weibull parameters, facilitating the calculation of the probability density function and the annual average wind speed. The findings were also compared with WAsP. A Student's *t*-Test showed that the energy pattern factor method closely matches the WAsP results. This method achieved a PDF correlation coefficient of 100% at reference height of 101 m and hub height of 80 m, respectively. The confidence level was above 97.5%. The key points of this research are summarized below.

(1) The local mean wind shear coefficient was 0.11, and the roughness parameter was 0.01 m, indicating that the terrain was open country with no structures or vegetation.
(2) The wind frequency results from Kaleidagraph and WAsP show that the prevailing wind direction was at 30° E of N, and the highest wind speed occurred in August 2007.
(3) Based on the Weibull parameters calculated from WAsP, it was found that the shape and scale factors at 80 m hub height were 2.73 and 9.10 m/s, respectively. This indicates that the annual average wind speed was 8.10 m/s, making the site suitable for IEC 61400-1 Edition 3 Class II wind turbine generators.
(4) The site's moderate wind potential was indicated by a measured average power potential of 368.53 W/m^2 at a height of 50 m (above ground level), classifying it as wind class 3 according to NREL's wind energy generation classification.
(5) The characteristic wind turbulence was also determined using standard deviation and turbulence intensity at a reference height of 101 m. The results calculated with the analytical method and Windographer software showed that the site was below Category C or IEC Subclass C.
(6) Among the wind turbine generators selected, the 2.5MW AV928 was chosen for having the lowest levelized energy cost of US$44.36/MWh, but with a maximum capacity factor of 41.22%.
(7) WAsP results revealed that the net annual energy yields considering the wake loss effects, for Phases I and II wind farms using 2.5 MW AV928 turbine generators were 104.92 GWh and 456.89 GWh, respectively.

5. Recommendation

This is a preliminary study of wind resource assessment in Santa Vitoria do Palmar, in the State of Rio Grande do Sul, Brazil. One year of wind data from 2007 to 2008 was used for analysis. To achieve a more reliable assessment, an updated set of wind data is needed to accurately determine the wind resource at the site. More recent data from Vortexfdc.com, using a newer version of WAsP and the full version of Windographer software, would be suitable for evaluating the wind resource.

Nomenclature

$\hat{b}$	absolute value of *y*-intercept
ρ	air mass density
T	ambient temperature
AEP	annual energy production
B	barometric pressure
C_f	capacity factor
C_{CapEx}	capital expenditures
$F(V)$	cumulative distribution function
R_0	dry air gas constant
FCR	fixed charge rate
Γ	gamma function
N_h	8760 h per year
$LCOE$	levelized cost of energy
W_{PD}	mean wind power density
V_m	mean wind speed
AEP_{Net}	net annual energy production
N	number of data points
C_{OpEx}	operational expenditures
$P(V)$	power output as a function of wind speed
$f(V)$	probability density function
E_{PF}	available wind power potential to the power proportional to the cube of average wind speed ratio
ϕ	relative humidity
A	scale factor
k	shape factor
σ	standard deviation
V_i	time-mean wind speed
P_w	vapor pressure
R_w	water vapor gas constant
α	wind shear coefficient

Author Contributions: G.L.A.: conceptualization, validation, investigation, project administration, supervision, methodology, software, original draft preparation; L.A.G.L.: formal analysis, investigation, writing—review and editing; K.L.: formal analysis, software, investigation, writing—review and editing. All authors have read and agreed to the published version of the manuscript.

Funding: This research received no external funding.

Institutional Review Board Statement: Not applicable.

Informed Consent Statement: Not applicable.

Data Availability Statement: The data that has been used is confidential.

Conflicts of Interest: The authors declare no conflict of interest.

Appendix A. WAsP Wind Turbine Cluster Report for 30 MW Phase I Wind Farm

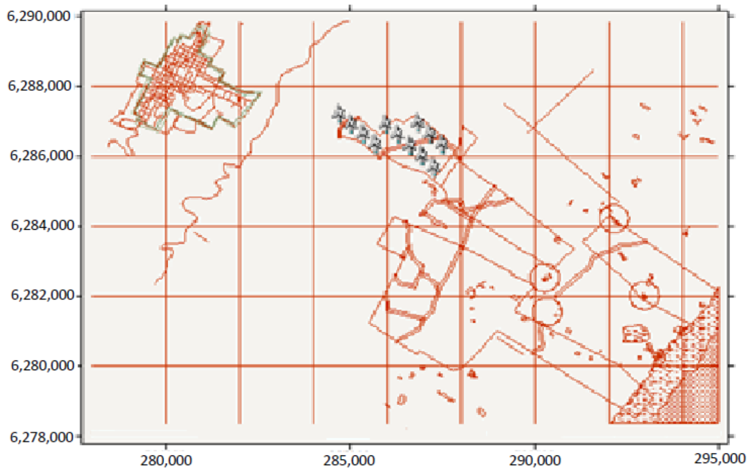

Figure A1. Wind turbine arrangement for 30 MW Phase I wind farm project in SVdP, Brazil.

Table A1. Gross and net annual energy yields for 30 MW Phase I wind farm in SVdP, Brazil.

Turbine	Location [m]	Gross AEP [MWh/Year]	Net AEP [MWh/Year]	Wake Loss [%]
Turbine site 01	(284728.1, 6286995.0)	9212.088	8936.961	2.99
Turbine site 02	(285064.1, 6286695.0)	9212.636	8835.006	4.10
Turbine site 03	(285399.1, 6286395.0)	9209.479	8718.673	5.33
Turbine site 04	(285734.2, 6286095.0)	9211.102	8683.431	5.73
Turbine site 05	(286008.4, 6286709.0)	9232.050	8704.259	5.72
Turbine site 06	(286321.6, 6286386.0)	9224.693	8578.385	7.01
Turbine site 07	(286648.6, 6286076.0)	9226.900	8550.640	7.33
Turbine site 08	(286975.5, 6285767.0)	9222.332	8623.599	6.49
Turbine site 09	(287302.4, 6285458.0)	9224.539	8910.134	3.41
Turbine site 10	(286886.0, 6286718.0)	9238.509	8713.291	5.69
Turbine site 11	(287220.6, 6286417.0)	9239.099	8732.709	5.48
Turbine site 12	(287547.3, 6286108.0)	9232.663	8928.198	3.30

Appendix B. WAsP Wind Turbine Cluster Report for 137.5 MW Phase II Wind Farm

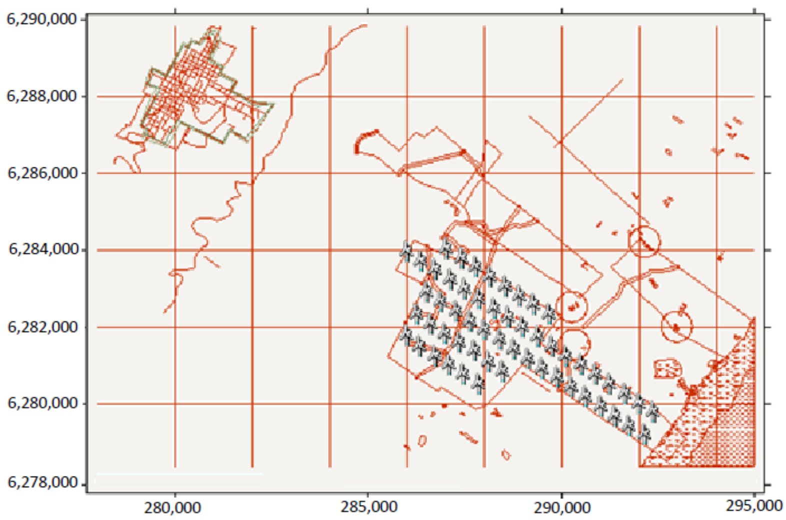

Figure A2. Wind turbine arrangement for 137.5 MW Phase II wind farm project in SVdP, Brazil.

Table A2. Gross and net annual energy yields for 137.5 MW Phase II wind farm in SVdP, Brazil.

Turbine	Location [m]	Gross AEP [MWh/Year]	Net AEP [MWh/Year]	Wake Loss [%]
Turbine site 01	(287,071.2, 6,283,827.0)	9207.682	8580.919	6.81
Turbine site 02	(287,447.3, 6,283,580.0)	9210.499	8477.827	7.95
Turbine site 03	(287,823.9, 6,283,334.0)	9221.178	8447.352	8.39
Turbine site 04	(288,200.6, 6,283,088.0)	9226.585	8434.600	8.58
Turbine site 05	(288,577.2, 6,282,842.0)	9229.091	8435.549	8.60
Turbine site 06	(288,953.8, 6,282,595.0)	9230.909	8449.457	8.47
Turbine site 07	(289,330.5, 6,282,349.0)	9232.227	8485.038	8.09
Turbine site 08	(289,707.1, 6,282,103.0)	9234.719	8630.596	6.54
Turbine site 09	(286,038.4, 6,283,759.0)	9250.590	8802.360	4.85
Turbine site 10	(286,412.8, 6,283,509.0)	9251.670	8572.858	7.34
Turbine site 11	(286,788.4, 6,283,262.0)	9252.472	8303.590	10.26
Turbine site 12	(287,164.0, 6,283,014.0)	9215.178	8072.240	12.40
Turbine site 13	(287,539.7, 6,282,766.0)	9219.386	8001.231	13.21
Turbine site 14	(287,915.3, 6,282,518.0)	9224.002	7973.580	13.56
Turbine site 15	(288,291.0, 6,282,271.0)	9229.795	7982.104	13.52
Turbine site 16	(288,666.6, 6,282,023.0)	9223.746	8022.271	13.12
Turbine site 17	(289,042.3, 6,281,775.0)	9235.461	8093.817	12.36
Turbine site 18	(289,417.9, 6,281,527.0)	9237.012	8225.919	10.95
Turbine site 19	(289,793.6, 6,281,279.0)	9238.179	8435.849	8.68
Turbine site 20	(290,169.2, 6,281,032.0)	9239.405	8537.174	7.60
Turbine site 21	(290,544.9, 6,280,784.0)	9240.371	8569.551	7.26
Turbine site 22	(290,920.5, 6,280,536.0)	9241.439	8593.782	7.01
Turbine site 23	(291,296.2, 6,280,288.0)	9243.009	8621.202	6.73
Turbine site 24	(291,671.8, 6,280,041.0)	9243.731	8658.562	6.33
Turbine site 25	(292,047.5, 6,279,793.0)	9244.422	8734.113	5.52
Turbine site 26	(292,423.1, 6,279,545.0)	9245.067	8941.527	3.28
Turbine site 27	(286,550.9, 6,282,688.0)	9241.870	8134.480	11.98
Turbine site 28	(286,927.4, 6,282,441.0)	9246.421	7952.039	14.00
Turbine site 29	(287,302.7, 6,282,193.0)	9251.367	7886.965	14.75
Turbine site 30	(287,678.0, 6,281,945.0)	9252.258	7865.086	14.99
Turbine site 31	(288,053.2, 6,281,696.0)	9253.081	7887.000	14.76
Turbine site 32	(288,428.5, 6,281,448.0)	9253.730	7965.344	13.92
Turbine site 33	(288,803.8, 6,281,200.0)	9231.600	8035.076	12.96
Turbine site 34	(289,179.1, 6,280,952.0)	9232.611	8172.564	11.48
Turbine site 35	(289,554.4, 6,280,703.0)	9233.454	8306.656	10.04
Turbine site 36	(289,929.7, 6,280,455.0)	9235.045	8379.324	9.27
Turbine site 37	(290,305.0, 6,280,207.0)	9237.364	8421.603	8.83
Turbine site 38	(290,680.3, 6,279,958.0)	9239.987	8450.535	8.54
Turbine site 39	(291,055.6, 6,279,710.0)	9242.360	8479.310	8.26
Turbine site 40	(291,430.9, 6,279,462.0)	9243.800	8527.894	7.74
Turbine site 41	(291,806.2, 6,279,213.0)	9243.747	8617.906	6.77
Turbine site 42	(292,181.5, 6,278,965.0)	9244.769	8890.795	3.83
Turbine site 43	(286,286.4, 6,282,126.0)	9233.396	8145.935	11.78
Turbine site 44	(286,650.3, 6,281,861.0)	9237.664	7975.045	13.67
Turbine site 45	(287,027.4, 6,281,616.0)	9239.759	7930.958	14.16
Turbine site 46	(287,404.8, 6,281,374.0)	9242.435	7915.095	14.36
Turbine site 47	(287,782.3, 6,281,149.0)	9243.915	7944.716	14.05
Turbine site 48	(288,159.7, 6,280,881.0)	9244.847	8055.596	12.86
Turbine site 49	(288,537.1, 6,280,636.0)	9247.471	8255.985	10.72
Turbine site 50	(286,027.2, 6,281,562.0)	9225.317	8319.907	9.81
Turbine site 51	(286,378.2, 6,281,280.0)	9229.637	8223.053	10.91
Turbine site 52	(286,755.4, 6,281,035.0)	9232.977	8196.278	11.23
Turbine site 53	(287,133.5, 6,280,791.0)	9234.858	8201.771	11.19
Turbine site 54	(287,511.6, 6,280,547.0)	9240.038	8253.039	10.68
Turbine site 55	(287,889.8, 6,280,303.0)	9241.982	8418.448	8.91

References

1. Nugent, D.; Sovacool, B.K. Assessing the lifecycle greenhouse gas emissions from solar PV and wind energy: A critical meta-survey. *Energy Policy* **2014**, *65*, 229–244.
2. IRENA. *Renewable Capacity Statistics 2025*; International Renewable Energy Agency: Abu Dhabi, United Arab Emirates.
3. Pereira, E.B.; Martins, F.R.; Pes, M.P.; et al. The impacts of global climate changes on the wind power density in Brazil. *Renew Energy* **2013**, *49*, 107–110.
4. Hayashi, T.; Liu, W.; Sassa, K. A preliminary investigation of low-cost SODAR anemometry. *Wind. Eng.* **2003**, *27*, 285–297.

5. Ormel, F.T.; Herman, S.A.; Eecen, S.A. Comparative Measurements with SODAR Systems Correlation with Meteorological Masts for Onshore and Offshore. Available online: https://www.osti.gov/etdeweb/biblio/20376551 (access on 19 June 2025).
6. Chaurasiya, P.K.; Warudkar, V.; Ahmed, S. An onsite demonstration and validation of LiDAR technology for wind energy resource assessment. *Int. J. Sustain. Energy* **2019**, *38*, 701–715.
7. Asian Development Bank. *Guidelines for Wind Resources Assessment: Best Practices for Countries Initiating Wind Development*; Asian Development Bank: Mandaluyong City, Philippines, 2014; pp. 1–49.
8. de Araujo Lima, L.; Bezerra Filho, C.R. Wind resource evaluation in São João do Cariri (SJC)—Paraiba, Brazil. *Renew. Sustain. Energy Rev.* **2012**, *16*, 474–480.
9. Silva dos Santos, A.T.; Santos e Silva, C.M.; Faro do Amaral Lemos, D.; et al. Assessment of wind resources in two parts of Northeast Brazil with the use of numerical models. *Meteorol. Appl.* **2016**, *23*, 563–573.
10. González MO, A.; Santiso, A.M.; de Melo, D.C.; et al. Regulation for offshore wind power development in Brazil. *Energy Policy* **2020**, *145*, 111756.
11. Vinhoza, A.; Schaeffer, R. Brazil's offshore wind energy potential assessment based on a Spatial Multi-Criteria Decision Analysis. *Renew. Sustain. Energy Rev.* **2021**, *146*, 111185.
12. Dos Reis, M.M.L.; Mazetto, B.M.; Da Silva, E.C.M. Economic analysis for implantation of an offshore wind farm in the Brazilian coast. *Sustain. Energy Technol. Assess.* **2021**, *43*, 100955.
13. *IEC 61400-1*; International Standard Norme Internationale Wind Turbines-Part 1: Design Requirements Eoliennes-Partie 1: Exigences de Conception. International Electrotechnical Commission: Geneva, Switzerland, 2005.
14. *IEC 61400-12-1*; International Standard IEC 61400-12-1 Wind Turbines Part 12-1: Power Performance Measurements of Electricity Producing Wind Turbines. International Electrotechnical Commission: Geneva, Switzerland, 2005.
15. Mathew, S. *Wind Energy: Fundamentals, Resource Analysis and Economics*; Springer: Berlin, Germany, 2006.
16. Veritas, D.N. *Guidelines for Design of Wind Turbine*; Jydsk Centraltrykkeri: Viby, Denmark, 2002.
17. Germanischer Lloyd, GL. *Guideline for the Certification of Wind Turbine 2003 with Supplement 2004*; Germanischer Lloyd, GL: Hamburg, Germany, 2003.
18. Bowden, G.J.; Barker, P.R.; Shestopal, V.O.; et al. The Weibull distribution function and wind statistics. *Wind. Eng.* **1983**, *7*, 85–98.
19. Kreyszig, E. *Advanced Engineering Mathematics*; John Wiley & Sons, Inc.: Boston, MA, USA, 2011.
20. Balouktsis, A.; Chassapis, D.; Karapantsios, T.D. A nomogram method for estimating the energy produced by wind turbine generators. *Sol. Eng.* **2002**, *72*, 251–259.
21. Mengelkamp, H.T. On the energy output estimation of wind turbines. *J. Energy Res.* **1988**, *12*, 113–123.
22. Chang, T.J.; Wu, Y.T.; Hsu, H.Y.; et al. Assessment of wind characteristics and wind turbine characteristics in Taiwan. *Renew. Energy* **2003**, *28*, 851–871.
23. Stevens, M.J.M.; Smulders, P.T. The Estimation of the Parameters of the Weibull Wind Speed Distribution for Wind Energy Utilization Purposes. *Wind. Eng.* **1979**, *3*, 132–145.
24. Hulio, Z.H.; Jiang, W. An assessment of effects of non-stationary operational condition on wind turbine under different wind scenario. *J. Eng. Des. Technol.* **2020**, *18*, 102–121.
25. Hulio, Z.H. Assessment of Wind Characteristics and Wind Power Potential of Gharo, Pakistan. *J. Renew. Energy* **2021**, *2021*, 8960190.
26. NREL. *2022 Cost of Wind Energy Review*; NREL: Washington, DC, USA, 2023.